Food Chemistry: X 22 (2024) 101432

Contents lists available at ScienceDirect

Food Chemistry: X

journal homepage: www.sciencedirect.com/journal/food-chemistry-x

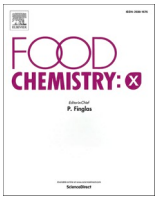

Volatolomics-assisted characterization of the key odorants in green off-flavor black tea and their dynamic changes during processing

Yanqin Yang [a], Jialing Xie [a], Qiwei Wang [a], Lilei Wang [a], Yan Shang [b], Yongwen Jiang [a,*], Haibo Yuan [a,*]

[a] Key Laboratory of Biology, Genetics and breeding of Special Economic Animals and Plants, Ministry of Agriculture and Rural Affairs, Tea Research Institute, Chinese Academy of Agricultural Sciences, Hangzhou 310008, China
[b] Hangzhou Zhishan Tea Industry Co., LTD, Hangzhou 310000, China

ARTICLE INFO

Keywords:
Green off-flavor
Black tea
GC-*E*-nose
GC-IMS
GC–MS
GC-O-MS

ABSTRACT

Aroma plays a pivotal role in the quality of black tea. However, the acceptability of black tea is greatly limited by the green off-flavor (GOF) resulting from the inappropriate processing control. In this study, the key odorants causing GOF were investigated by volatolomics, and their dynamic changes and formation pathways were in-depth understood. Significant alterations in volatile metabolites were observed in the withering stage. A total of 14 key odorants were identified as contributors to GOF, including 2-methylpropanal, 3-methylbutanal, 1-hexanol, nonanal, *(E, E)*-2,4-heptadienal, benzaldehyde, linalool, *(E, E)*-3,5-octadiene-2-one, *β*-cyclocitral, phenylacetaldehyde, *(E, E)*-2,4-nonadienal, methyl salicylate, geraniol, and *β*-ionone. Among them, *(E, E)*-2,4-heptadienal (OAV = 3913), characterized by fatty, green, and oily aromas, was considered to be the most important contributor causing GOF. Moreover, it was found that lipid degradation served as the primary metabolic pathway for GOF. This study provides a theoretical foundation for off-flavor control and quality improvement of black tea.

1. Introduction

As a fully fermented tea, black tea is the second most consumed tea after green tea among six kinds of tea in China. It is favored by consumers due to its captivating flavor and diverse health benefits such as anti-inflammatory, anti-cancer, antioxidant, and hypoglycemic effects (Yang, Hua, et al., 2020). Typically, the manufacturing processes of black tea mainly include withering, rolling, fermentation, and drying, each of which has an important effect on the flavor quality of black tea (Yang, Wang, et al., 2024). To date, numerous studies have primarily focused on the effect of the processing technology on charming flavor, such as floral aroma, fruity aroma, sweet fragrance, etc. (Chen, Yang, et al., 2022; Yang, Hua, et al., 2020). For instance, researchers have extensively delved into the dynamic changes of volatile and non-volatile metabolites in sweet aroma black tea throughout the processing stages (Yang, Xie, et al., 2024). Green off-flavor (GOF), also known as greenish odor, is described as a particularly unpleasant odor that smells like uncooked green vegetables. And it is mainly caused by inappropriate processing control. Nevertheless, to date, details regarding the key odorants responsible for the defective flavor in black tea have been seldom investigated. Additionally, the dynamic changes and formation mechanisms of defective flavor during processing remain poorly understood, hampering both quality enhancement and technological improvements in black tea production. At the same time, it is also a key technical bottleneck restricting the high-quality development of the black tea industry.

Aroma is one of the important factors to evaluate the quality of tea, which greatly affects consumers' purchase desire and acceptance. At present, tea aroma mainly relies on the sensory evaluation of experts, leading to subjective differences and poor repeatability. Rapid and objective instrumental analysis is urgently needed. By mimicking the human olfactory system, the electronic nose (e-nose) is capable of recognizing a variety of odors for volatile profile characterization. Unlike traditional e-nose based metal oxide sensors, which is prone to signal drift and contamination, gas chromatography-based electronic nose (GC-*E*-Nose) combines the benefits of sensor technology and fast gas chromatography to provide more volatile information (Xie et al., 2023; Yang, Hua, et al., 2020). Gas chromatography-mass spectrometry

* Corresponding author.
E-mail addresses: jiangyw@tricaas.com (Y. Jiang), 192168092@mail.tricaas.com (H. Yuan).

https://doi.org/10.1016/j.fochx.2024.101432
Received 17 March 2024; Received in revised form 16 April 2024; Accepted 29 April 2024
Available online 1 May 2024

(GC–MS) has been widely used in the flavor analysis due to its excellent qualitative and quantitative capabilities (Rong et al., 2023; Yang et al., 2018; Yang, Zhang, et al., 2020). Nevertheless, advanced analytical techniques for distinguishing low-concentration flavor components from highly complex tea samples are still sought after. As a promising analytical technique, gas chromatography-ion mobility spectrometry (GC-IMS) can work under ambient pressure and temperature, with the advantages of simple operation, extraordinary sensitivity (ppb level), good selectivity and easy miniaturization (Wang et al., 2023). Moreover, it offers the advantage of visualizing the differences between samples with color contour images. Currently, GC-IMS has been successfully applied to distinguish different flavors of black tea and characterize the processing process of chestnut-like aroma green tea (Yang et al., 2022; Yang, Qian, Deng, Yuan, & Jiang, 2022). To date, more than 700 volatile compounds have been reported in tea. Only a small number of volatile components have aroma activity and are responsible for the overall aroma characteristics of tea. Gas chromatography-olfactometry-mass spectrometry (GC-O-MS) technique is a useful tool for exploring the key aroma-active substances and has been extensively utilized in the flavor analysis of various tea samples (Li et al., 2023; Uselmann & Schieberle, 2015; Zhao et al., 2022).

As a new field of metabolomics, volatolomics employs various analytical techniques to qualitatively and quantitatively characterize the volatile metabolites in targeted samples (Chen et al., 2023; Wang et al., 2023; Yang, Wang, et al., 2024). In view of the variability and complexity of volatile components in tea, it is of great significance to comprehensively characterize the aroma characteristics by integrating various flavor analysis techniques. The aim of this study was to investigate the dynamic changes of volatile profiles of GOF black tea during processing by a combination of GC-*E*-Nose, GC-IMS, and GC–MS. Furthermore, the key odorants responsible for the GOF were screened using the odor activity value (OAV) and GC-O-MS. The possible formation pathways of these key odor components were elucidated. The results expand our understanding on the formation of the off-flavor and lay a theoretical foundation for off-flavor control and enhancement in black tea.

2. Materials and methods

2.1. Samples and chemicals

The fresh leaves (FL) were collected from Shengzhou, Zhejiang Province, in mid-April 2021. All the samples were made from *Camella sinensis cv.* 'Jiukeng' with one-bud-one-leaf to one-bud-two-leave. The typical processing processes encompassed withering, rolling, fermentation, first drying, and final firing, and the specific process parameters were shown in Fig. S1. The processed samples were freeze-dried in a vacuum freeze-dryer and then stored at −20 °C in the refrigerator along with the finished tea for subsequent analysis.

Ethyl decanoate was purchased from TCI Chemical Industry Development Co., Ltd. (Shanghai, China). Purified water was obtained from Hangzhou Wahaha Group Co., Ltd. (Hangzhou, China). The *n*-alkane (C7-C40) mixtures were purchased from sigma-Aldrich (Shanghai, China). Headspace vials (20 mL) were obtained from Agilent Technologies Inc. (Palo Alto, CA, U.S.A). The *n*-ketones (C4-C9) were purchased from Sinopharm Chemical Reagent Beijing Co., Ltd. (Beijing, China). The information of standard substances used in this study were listed in Table S1.

2.2. Sensory evaluation

The tea samples were accessed in accordance with GB/T 23776–2018, and ethical permission was not required. The finished black tea samples underwent evaluation by 5 experienced experts who gave their consent to take part and use their information (2 females and 3 males, aged between 30 and 55 years old) with the title of senior tea assessor. To be specific, 3 g of tea samples were put into a white porcelain cup, and 150 mL of boiling water was added and brewed for 5 min, then the infusion was strained out. A percentage system was used for evaluation, in which appearance, liquor color, aroma, taste and infused leaf accounted for 20%, 10%, 25%, 30% and 10%, respectively. The results of sensory evaluation were listed in Table S2. By repeated confirmation, the aroma of the finished black tea samples was defined as green off-flavor.

2.3. Gas chromatography electronic nose analysis

The volatile fingerprints of GOF black tea during processing were carried out on a Heracles II GC-*E*-Nose (Alpha M.O.S., Toulouse, France). Detailed parameters for analysis were referenced from previous studies with minor modification (Yang, Wang, et al., 2024). Briefly, tea samples (0.5 g) and purified water (3 mL) were introduced into a 20-mL headspace vial with an incubation temperature of 65 °C and incubation duration of 30 min. The agitation speed was 500 rpm. A total of 5000 μL headspace was introduced into the injection port system at an injection rate of 250 μL/s. Volatile compounds were trapped at 40 °C for 55 s using a Tenax TA trap, followed by thermal desorption at 240 °C for 30 s. Two different polarity columns (MXT-5 and MXT-1701, 20 m × 0.18 mm × 0.4 μm, Restek, USA) were used to separate the volatile compounds. The temperature program was as follows: maintained at 50 °C for 2 s, then ramped to 80 °C with a rate of 0.2 °C /s, and finally increased to 250 °C at a rate of 0.8 °C /s (holding for 96 s). The temperature of two flame ionization detectors (FIDs) was set at 260 °C and the gain factor was set to 12. The length of the entire analysis was 460 s. All analyses were performed in triplicate.

2.4. Gas chromatography-ion mobility spectrometry analysis

A commercial GC-IMS instrument (Flavourspec®, G.A.S, Dortmund, Germany) was used to analyze the fingerprint of GOF black tea at different processing stages. The analysis conditions were referred to our previous studies (Yang, Xie, et al., 2024). Specifically, accurately weighed 1.0 g of tea samples were placed into a sealed 20-mL headspace vial and incubated at 60 °C for 15 min with a shaking speed of 500 rpm. After the incubation process, 500 μL of headspace was injected into the injection port through a syringe heated at 85 °C. An MXT-5 capillary column (15 m × 0.53 mm × 1 μm, Restek, Beijing, China) was performed for volatile component separation, and the column temperature was set at 60 °C. High-purity nitrogen (99.999%) was employed as carrier gas. The programmed flow rate was set as follows: 2 mL/min ranged from 0 min to 2 min and 100 mL/min ranged from 2 min to 20 min. The temperature of the drift tube was set at 45 °C, and the flow rate of the drift gas (N_2, 99.999%) in the drift tube was 150 mL/min. Each sample was subjected to analysis in triplicate.

The retention index (RI) of GOF black tea was calculated using *n*-ketone C4-C9 mixtures as the IMS did not react to alkanes. The volatile compounds were qualitatively analyzed based on the RI and the normalized drift time compared with those of standards in the GC-IMS database. The GC-IMS spectrograms were processed by using the *Laboratory Analytical Viewer*. The topographic maps were constructed by the *Reporter plug-in* while differential fingerprints were recorded by the *Gallery Plot plug-in*.

2.5. Gas chromatography-mass spectrometry analysis

The volatile compounds were analyzed on an Agilent 7890B GC coupled to a 7000C mass spectrometry system (Agilent Technologies, Palo Alto, CA, U.S.A.). Briefly, 0.5 g of tea samples were placed into a 20-mL headspace vial, accompanied by 5 mL of boiling water and 2 μL of ethyl decanate (100 mg/L, internal standard). After incubation at 60 °C for 60 min, the divinylbenzene/carboxen/polydimethylsiloxane (DVB/CAR/PDMS, 50/30 μm; Supelco, USA) fiber was pulled out of the

headspace vial and then inserted into the injection port (about 250 °C) for thermal desorption (about 5 min). The volatile components were guided through an HP-5 ms capillary column (60 m × 250 μm × 0.25 μm; Agilent Technologies, Palo Alto, CA). High-purity helium (99.999%) was utilized as carrier gas at a flow rate of 1.0 mL/min in a split-less mode. The temperature program was initiated at 40 °C for 5 min, increased to 100 °C at 6 °C/min (holding for 2 min), and finally ramped to 270 °C at 5 °C/min (holding for 4 min). Electron ionization (EI) mode was employed, with a scanning range of 33–550 *m/z*. The ion source temperature was set at 230 °C and the transmission line temperature was set at 270 °C.

Qualitative analysis was conducted using Agilent MassHunter workstation software Unknowns analysis. Volatile compounds were identified by comparison with mass spectrometry of NIST11.0 library, standard certification and RI calculated from a homologous series of *n*-alkanes (C7-C40). The volatile components were accurately quantified by standard curves, and the qualitative and quantitative ion pairs and standard curve information were listed in Table S3. Some volatiles without commercially available standards were quantified by the ratio of peak area between targeted compound and internal standard (ethyl decanoate).

2.6. Calculation of odor activity values

Odor activity value (OAV) refers to the ratio of a compound's content to its threshold value, which can be calculated by the following formula: $OAV_i = C_i/OT$, where C signifies the volatile compound's content, and OT denotes its corresponding odor threshold. In general, aroma compounds with OAVs greater than or equal to 1 are typically deemed potential contributors to the overall aroma (Xiao et al., 2022; Zhang et al., 2020).

2.7. Gas chromatography-olfactometry-mass spectrometry analysis

The aroma-active compounds in GOF black tea were analyzed by an Agilent 7890A GC coupled to an Agilent 5975C mass spectrometer (Agilent, Palo Alto, CA, USA) equipped with a sniffing detector port (ODP4, Germany). The effluents were split between the sniffing port and MS detector at a ratio of 1:1. A HP-Innowax column (60 m × 0.25 mm × 0.25 μm; Agilent, Palo Alto, CA, USA) was used for aroma separation. Briefly, the program temperature was as follows: initially at 40 °C for 2 min, increased to 250 °C at a rate of 5 °C /min, holding for 20 min.

The sniffing experiment was conducted by a highly trained sensory panel consisting of 5 professional sensory evaluators assessors (2 females and 3 males, aged between 30 and 55 years old). The sniffing process was carried out independently by each panelist and the aroma properties and intensity were recorded. The aroma intensity (AI) was ranged from 1.0 to 4.0, where "1.0" represented weak, "2.0" represented medium, "3.0" represented strong, and "4.0" represented extremely strong.

2.8. Statistical analysis

All experimental samples were analyzed three times, and the data were expressed as mean value ± standard deviation. *SPSS* statistics 20.0 (SPSS Inc., Chicago, IL, USA) was used for one-way analysis of variance (ANOVA) followed by Duncan's multiple comparison tests. Partial least squares discriminant analysis (PLS-DA) and orthogonal PLS-DA (OPLS-DA) were conducted utilizing SIMCA 14.1 (Umetrics, Sweden). The bar chart was plotted with Origin 9.1 (Origin Lab Corporation, Northampton, USA). The heat map was constructed with the MultiExperiment Viewer 4.9.0 (Oracle Corporation, Redwood Shores, USA).

3. Results and discussion

3.1. Volatile fingerprints of GOF black tea during processing by GC-E-Nose

In recent years, food flavor is developing towards non-destructive direction. In contrast to the conventional sensor-array electronic noses, the GC-E-Nose, which amalgamates the advantages of electronic nose technology with gas chromatography, has drawn attention for its streamlined operation, rapid analysis, and real-time monitoring (Chen, Yang, et al., 2022; Wei, Dan, Zhao, & Wang, 2023). Moreover, the built-in data processing system enables swift and diverse characterization of volatile fingerprints. In this study, the volatile fingerprints of finished black tea with GOF were depicted in Fig. S2[A]), accompanied by the corresponding radar map in Fig. S2[B]). Generally, the peak responses from the MXT-5 column surpassed those from the MXT-1701 column.

To comprehend the dynamic alterations of volatile fingerprints during processing, OPLS-DA was employed. As a supervised statistical method of discriminant analysis, OPLS-DA utilizes partial least squares regression to establish a model linking metabolite expression with sample classification. This approach integrates orthogonal signal correction (OSC) and PLS-DA technique to sift out differential variables by eliminating irrelevant discrepancies. As two important parameters (R^2Y and Q^2) of OPLS-DA model, the closer the value of R^2Y is to 1, the higher the interpretation rate of the Y matrices. Typically, Q^2 around 0.5 serves as a benchmark to assess the performance of model. In this study, the OPLS-DA model exhibited robust parameters, indicating a strong fit ($R^2Y = 0.987$) and high predictive power ($Q^2 = 0.91$) (Fig. 1[A]). The score plots of OPLS-DA model delineated dynamic changes in volatile fingerprints of GOF throughout the entire processing, distinctly

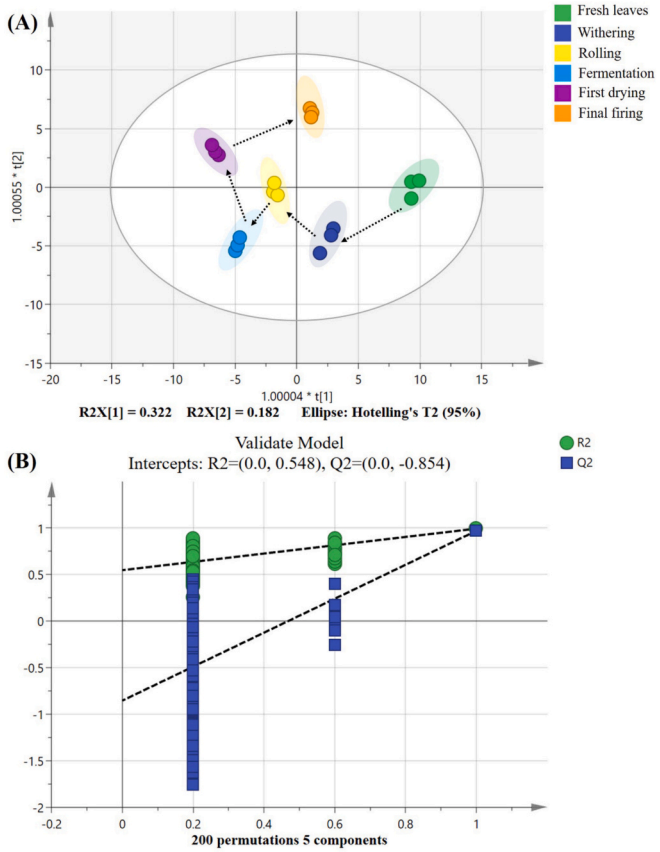

Fig. 1. The results of OPLS-DA obtained from GC-*E*-Nose. (A) The score plots of OPLS-DA ($R^2Y = 0.987$, $Q^2 = 0.91$); (B) Cross-validation by a 200-times permutation test ($R^2 = 0.548$, $Q2 = -0.854$).

distinguishing them at each stage. Notably, the volatile metabolites showcased significant changes during the withering and final firing stages. As a pivotal processing step of black tea, withering has a profound effect on the volatile substances through hydrolysis, oxidation, condensation and polymerization catalyzed by related endogenous enzymes (Fang, Liu, Xiao, Ma, & Huang, 2023). In addition, withering is not only a process of water loss, but also leads to changes in leaf tissue morphology and membrane permeability, thus augmenting the availability of enzymes required for subsequent processing (Liu, Chen, Sun, & Ni, 2022). As the key process of black tea, drying under high temperature instigates the Maillard reaction between sugars and amino acids, which in turn promotes the aroma formation (Yang, Hua, et al., 2020). In order to assess the reliability of model, a permutation test with 200 times was carried out. The parameters ($R^2 = 0.548$, $Q^2 = -0.854$) (Fig. 1 [B]) indicated that the model was robust, and no overfitting was observed. In summary, GC-*E*-Nose combined with multivariate statistical analysis could quickly characterize the alterations of volatile fingerprints during the processing of black tea.

3.2. Volatile fingerprints of GOF black tea during processing analyzed by GC-IMS

3.2.1. GC-IMS topographic plots of GOF black tea during processing

To unravel the change pattern of GOF black tea during processing, GC-IMS was employed to capture the comprehensive volatile profiles. The three-dimensional topographic maps of GOF black tea throughout the processing stages were illustrated in Fig. S3[A], allowing visual observation of the similarities and discrepancies in volatiles across different processing stages. The volatile profiles of GOF black tea in topographic maps were depicted in Fig. S3[B], where the ordinate signifies gas chromatographic retention time and the abscissa represents ion migration time. The red vertical line at an abscissa of 1.0 signifies the normalized reactive ion peak (RIP). The color of the topographic map generally denotes the signal intensity of volatile compounds, with red indicating higher concentration and white representing lower concentration. For better comparison, the spectral diagram of fresh leaves served as a reference, with the spectra of subsequent processing stage deducted from this reference. The deducted white background indicated equivalent content, while red and blue signified higher and lower concentrations compared to the reference, respectively. As shown in Fig. S3 [C], the retention time of most peak signals fell within the range of 100 to 400 s, with corresponding drift times spanning 1.0 to 1.8. Notably, as processing advanced, the distribution pattern of peak signals in GOF black tea remained consistent across different processing stages. However, varying signal intensities among samples suggested content variations in volatile substances. We postulate that the disparity during processing may derive from the complex biochemical reactions such as Maillard reaction, lipid degradation, and glycoside hydrolysis.

3.2.2. Volatile fingerprints of GOF black tea during processing

A total of 121 signal peaks were detected, among which 79 typical targeted compounds were identified (corresponding to 105 signal peaks) (listed in Table S4). These volatiles comprised 16 alcohols, 2 aromatic hydrocarbons, 3 sulfides, 23 aldehydes, 4 acids, 2 terpenes, 12 ketones, 7 heterocyclic groups, and 10 esters. Generally speaking, volatiles with heightened proton affinity or concentration exhibited a tendency to form dimers or polymers (Wan et al., 2023). Notably, 26 volatile compounds were found to be coexisted as monomers and dimers.

To identify subtle trends and differences of volatile compounds throughout the processing, the Gallery Plot plug-in was used to generate a visual fingerprint. Each row signifies the volatile compounds within the sample, while each column denotes the signal strength of volatile compounds across different samples. As shown in Fig. 2, the entire processing sequence was delineated into distinct regions—A, B, C, D, E, and F—for detailed analysis based on the fluctuation trends of volatile compounds. Noteworthy findings emerged at various processing stages: As for A region, thiophene, *o*-xylene, ethanol, 1-propanol monomer and dimer, pentanal, hexanal monomer and dimer, and *cis*-3-hexenyl acetate monomer and dimer exhibited higher contents in the fresh leaves compared to other stages. In B region, the contents of volatile compounds such as 1-heptanol, *(Z)*-3-hexenyl propanoate, 1-octen-3-one, 2-octanone, γ-terpinene, *(Z)*-2-pentenal dimer, and 4-methyl-3-penten-2-one monomer and dimer were higher in the withering stage than in other stages. As far as C region is concerned, significant enhancement was observed in the contents of 2-butanol monomer and dimer, tetrahydrofuran monomer and dimer, propyl acetate monomer and dimer, and 6-methyl-5-hepten-2-one in the rolling stage. In D region, aldehydes (such as *(E, E)*-2,4-octadienal, citronellal, phenylacetaldehyde, benzaldehyde monomer and dimer, octanal, heptanal monomer and dimer, *(E)*-2-octenal monomer and dimer, *(E)*-2-hexenal monomer and dimer, and *(Z)*-4-heptenal) and alcohols (such as linalool, linalool oxide, 1-octen-3-ol, *(Z)*-3-hexenol monomer and dimer, 1-hexanol monomer and dimer, and 3-pentanol) reached higher contents in the fermentation stage than other stages. It was reported that 1-octen-3-ol was formed from linoleic acid while heptanal originated from the oxidation degradation of oleic acid and palmitoleic acid. Monoterpene alcohols such as linalool and linalool oxide were liberated by hydrolyzing glycosidic bonds during the manufacturing process (Ho, Zheng, & Li, 2015). For the E region, the contents of 3-ethylpyridine, 3-methyl-2-butenal, 3-methylbutanal, butanal, and *(E)*-2-pentenal were found to be higher in the first firing stage than those in other stages. In regard to F region, representative compounds such as 2-pentylfuran, 2-ethylfuran, 2-butanone, 2-heptanone monomer and dimer, 3-methyl-2-pentanone, *cis*-2-penten-1-ol attained their peak levels in the final firing stage. The formation of 2-pentylfuran and 2-ethylfuran was potentially attributed to the Maillard reaction under high temperatures.

3.2.3. Multivariate statistical analysis

To better differentiate the variations of GOF black tea at distinct processing stages, an OPLS-DA was conducted on the volatile fingerprints. As shown in Fig. S4[A], satisfactory model parameters ($R^2Y = 0.986$, $Q^2 = 0.968$) were obtained. The score plots of OPLS-DA indicated that GOF black tea at different processing stages could be well distinguished. Notably, prominent separations were observed between “fresh leaves” and “withering” as well as “fermentation” and “first drying”. This underscored that the most substantial alterations in volatile components occurred during the withering and first drying processes compared to other stages. In addition, the reliability of model was confirmed via a permutation test of 200 iterations, displaying R^2 and Q^2 intercept values of (0, 0.17) and (0, −0.848), respectively. The Q^2 regression line was <0 at the ordinate intersection, indicating that the OPLS-DA model had strong robustness (Fig. S4[B]). These findings strongly resonate with the outcomes from GC-*E*-Nose analysis.

3.3. Dynamic changes of GOF black tea during processing analyzed via GC–MS

3.3.1. Characterization of volatile compounds in GOF black tea during processing

The volatile profiles of GOF black tea during processing were explored thoroughly via GC–MS analysis. As listed in Table S5, a total of 77 volatile compounds were identified through database search, retention index and standard certification. These volatiles were categorized into ten subclasses based on their chemical structures: 13 alcohols, 2 aromatic hydrocarbons, 2 phenols, 20 aldehydes, 1 acid, 10 ketones, 1alkane, 8 alkenes, 3 heterocyclic compounds, and 17 esters. Among them, the primary category was aldehydes, accounting for the highest proportion (25.97%), followed by esters (22.08%), alcohols (16.88%), and ketones (12.99%) (Fig. 3[A]). Distinctive variations were observed among the different categories of volatiles across the processing stages (Fig. 3[B]). Alcohols were presented at the highest level across all categories, ranging from 7978.52 μg/L (withering) to 13,623.32 μg/L

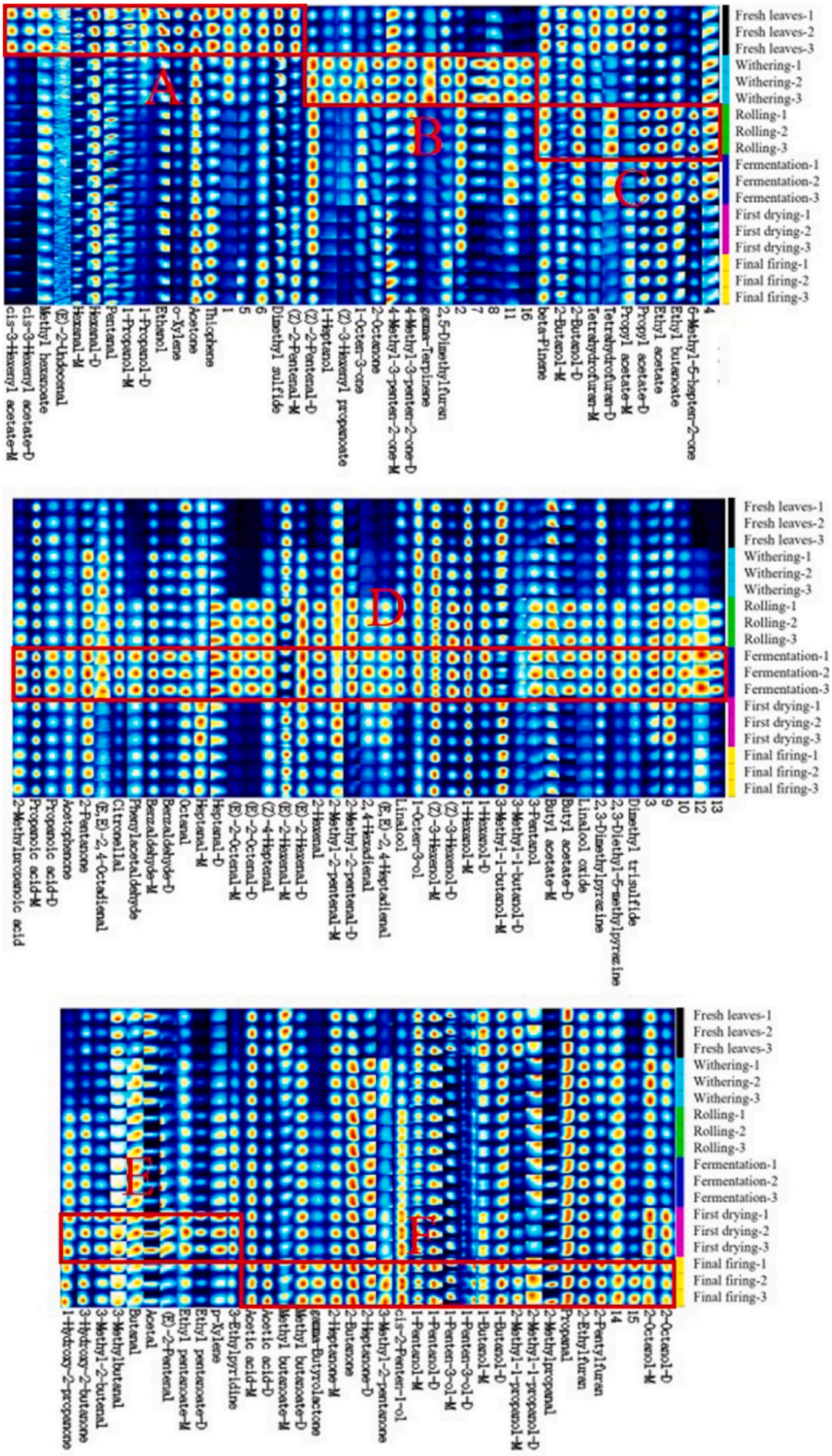

Fig. 2. Fingerprints of black tea with green off-flavor during processing generated by *Gallery Plot*. The suffix-M represented a monomer while the suffix-D represented a dimer. (For interpretation of the references to color in this figure legend, the reader is referred to the web version of this article.)

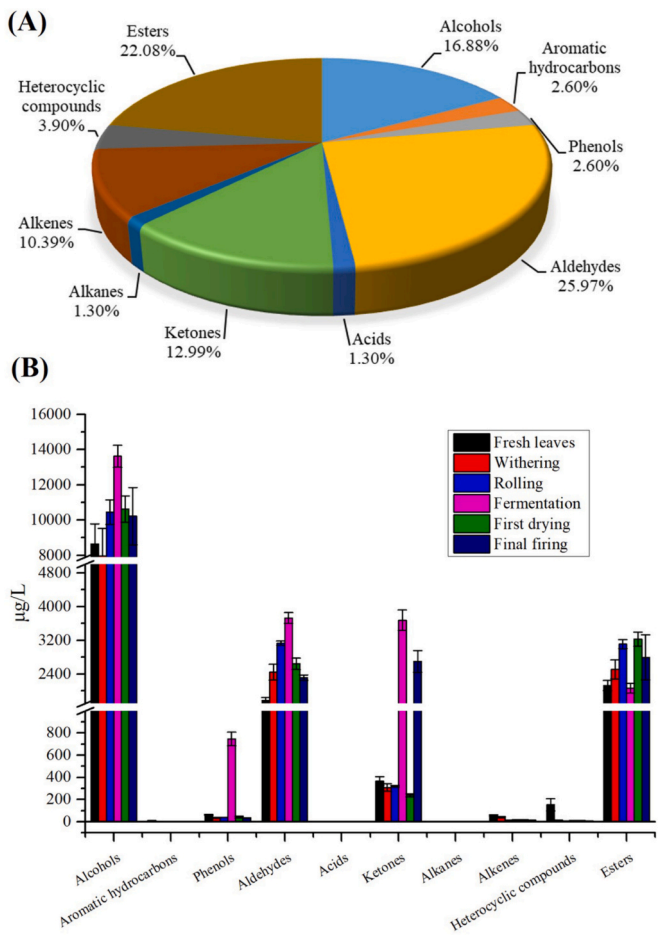

Fig. 3. Volatile components in GOF black tea during the entire manufacturing process obtained from GC–MS. (A) Percentages of different volatile categories; (B) Dynamic changes of different volatile categories during processing.

(fermentation). The results were partially consistent with previous studies (Liu et al., 2023). As for the aldehydes, the highest content was found in the fermentation stage (3729.30 μg/L), contrasting with the lowest content found in fresh leaves (1773.08 μg/L). Esters reached the highest content in the first drying stage (3230.58 μg/L) and exhibited their lowest level in the fermentation stage (2066.15 μg/L).

3.3.2. *Volatile variations in GOF black tea during processing*

For discovering the rule of dynamic change during processing, a PLS-DA model was constructed using 77 volatile components. The established model exhibited impressive parameters with $R^2Y = 0.98$ and $Q^2 = 0.915$, underscoring its exceptional explanatory and predictive capabilities (Fig. 4[A]). The score plots of PLS-DA visibly delineated separations between "fresh leaves" and "withering" as well as "withering" and "rolling", indicating substantial variations in volatile compounds at withering and rolling stages. To assess the potential overfitting, 200 permutation tests were conducted, yielding the intercepts of R^2 and Q^2 at 0.533 and −0.763, respectively (Fig. 4[B]). These values affirmed the reliability and robustness of model. Mirroring the findings from GC-*E*-Nose and GC-IMS, withering is emerged as a pivotal process significantly influencing the volatile compounds.

Furthermore, an exploration into the pivotal differential components in GOF black tea during processing were explored by variable importance in the projection (VIP). Typically, when the VIP value surpasses 1, it signifies a significant role in differentiation. In total, 34 differential metabolites were selected based on VIP > 1.0 (Fig. 4[C]). Additionally, employing VIP > 1.0 and one-way ANOVA ($p < 0.05$) as the threshold, 30 key differentiating components were screened out. Subsequently, heat map was constructed to visualize how these compounds changed throughout the processing stages. As depicted in Fig. 4[D], 6-methyl-5-heptene-2-one reached the maximum in fresh leaves. Some volatile components such as 2-heptanone, *(Z)*-3-hexen-1-yl (Z)-3-hexenoate, *α*-cyclocitral, methyl salicylate, decanal, *(E, E)*-2,4-decadienal, 2-methyl-2-butenal, *cis*-3-hexenyl isobutyrate, and hexanoic acid, hexyl ester reached higher levels at the withering stage compared to other processes. After the rolling stage, significant increase was observed in the content of 2-methylpropanal. As for the fermentation processing is concerned, the contents of *β*-cyclocitral, benzaldehyde, and 2-methoxyphenol were found to be higher than other processes. Compared with other stages, the first drying process was seen to be higher in the contents of geraniol, benzoic acid, ethyl ester, *(E)*-2-pentenal, and 1-penten-3-ol. The final firing contributed to the accumulations of *β*-ionone and nerolidol.

3.3.3. *Identification of the key odorants in finished GOF black tea by OAV and GC-O-MS analysis*

The aroma profiles of tea are the comprehensive effects of aroma components according to different proportions and concentrations, and the contribution degree of identified aroma-active substances to the overall aroma mainly depends on their content and corresponding odor threshold. Typically, volatiles with OAV ≥ 1 are considered to be the most potent contributors responsible for the overall aroma profile (Yin et al., 2023). As listed in Table S6, a total of 28 active-aroma compounds in finished GOF black tea were identified by OAV analysis. Specifically, the representative compounds mainly encompassed 15 aldehydes (2-methylpropanal, 3-methylbutanal, heptanal, benzaldehyde, *(E, E)*-2,4-heptadienal, phenylacetaldehyde, nonanal, *α*-cyclocitral, *(E, Z)*-2,6-nonadienal, *(E)*-2-nonenal, decanal, *β*-cyclocitral, *(E, E)*-2,4-nonadienal, citral, and *(E, E)*-2,4-decadienal), 7 alcohols (1-penten-3-ol, 1-hexanol, 1-octen-3-ol, 1-octanol, linalool, phenylethyl alcohol, and geraniol), 5 ketones (1-octen-3-one, *(E, E)*-3,5-octadien-2-one, *β*-damascone, *cis*-jasmone and *β*-ionone) and 1ester (methyl salicylate). Notably, *(E, E)*-2,4-heptadienal (OAV = 3913) emerged as the foremost important odorant, followed by *β*-ionone (OAV = 1873) and *(E, Z)*-2,6-nonadienal (OAV = 1223).

In addition, GC-O-MS analysis was used to characterize the active-aroma components in GOF black tea. A total of 30 active-aroma compounds were identified, belonging to 7 chemical classes: aldehydes (17), ketones (6), alcohols (3), phenol (1), alkene (1), heterocyclic compound (1) and ester (1) (listed in Table S7). Aldehydes accounted for the largest proportion, up to 56.67%, and these aldehydes are typically recognized for exhibiting fresh, greenish and fatty odors (Guo, Schwab, Ho, Song, & Wan, 2022). The representative aldehydes mainly encompassed 2-methylpropanal, 2-methylbutanal, 3-methylbutanal, pentanal, hexanal, 2-methyl-2-butenal, *(E)*-2-pentenal, *(E)*-2-hexenal, *(E)*-2-heptenal, nonanal, *(E)*-2-octenal, *(E, E)*-2,4-heptadienal, benzaldehyde, *β*-cyclocitral, phenylacetaldehyde, *(E, E)*-2,4-nonadienal, and geranial. Ketones, associated with floral, sweet, and fruity flavors, included volatiles like 3-hexanone, 3-methyl-2-pentanone, 3-nonen-2-one, *(E, E)*-3,5-octadiene-2-one, *β*-ionone, and *γ*-nonalactone. Alcohols such as linalool and geraniol exhibited rose-like and sweet flavors while hexanol was linked to green and fat odors. Additionally, eugenol, *β*-ocimene, 2-ethylfuran, and methyl salicylate were also sniffed, suggesting potential contributions to the GOF.

As mentioned above, the aroma-active components identified by OAV calculation and GC-O-MS revealed inconsistencies, potentially attributed to the variations in odor thresholds reported in different literature sources and the subjective factors inherent in the GC-O-MS sniffing process. By integrating both methods, the identification of aroma-active components could mitigate these respective limitations. Consequently, based on the common components identified by these two methods, 14 key volatiles, including 2-methylpropanal, 3-methylbutanal, 1-hexanol, nonanal, *(E, E)*-2,4-heptadienal, benzaldehyde,

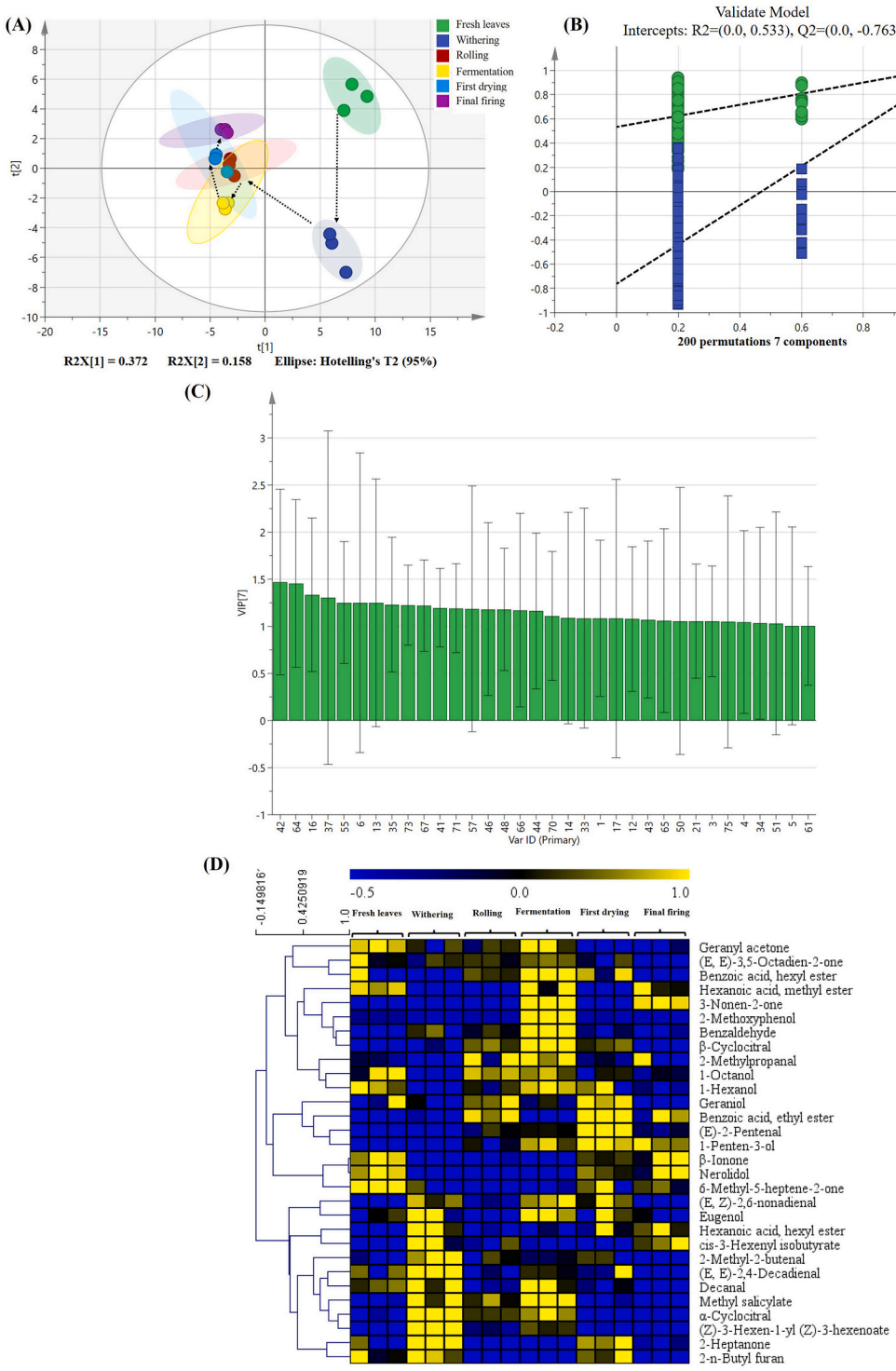

Fig. 4. Multivariate statistical analysis of GOF black tea during the entire manufacturing process. (A) Score plots of PLS-DA ($R^2Y = 0.98$, $Q^2 = 0.915$); (B) Cross-validation by 200-times permutation test ($R^2 = 0.533$, $Q^2 = -0.763$); (C) Volatiles with VIP > 1.0 (The compound numbers corresponded to Table S5); (D) Heatmap visualization constructed with the differential volatiles (VIP > 1.0 and $p < 0.05$).

linalool, *(E, E)*-3,5-octadiene-2-one, *β*-cyclocitral, phenylacetaldehyde, *(E, E)*-2,4-nonadienal, methyl salicylate, geraniol, and *β*-ionone were selected to be the most definitive odorants responsible for GOF (Fig. 5).

3.3.4. *Analysis of the formation pathways of key odorants in GOF black tea*

Drawing upon the classical metabolic pathways of volatile compounds in tea, the degradation or transformation pathways of key odorants were elucidated. According to the types of volatile precursor substances, it could be correspondingly divided into four categories: 5 fatty acid-derived volatiles (FADVs), 4 glycoside-derived volatiles (GDVs), 3 amino acid-derived volatiles (AADVs), and 2 carotenoid-derived volatiles (CDVs) (Chen, Zhu, et al., 2022; Zhou, He, & Zhu, 2023). Notably, the FADVs appeared to be the most abundant, implying that lipid degradation played a pivotal role in the formation of GOF.

Among these pathways, *β*-cyclocitral and *β*-ionone were representative odorants derived from *β*-carotene degradation. It is worth

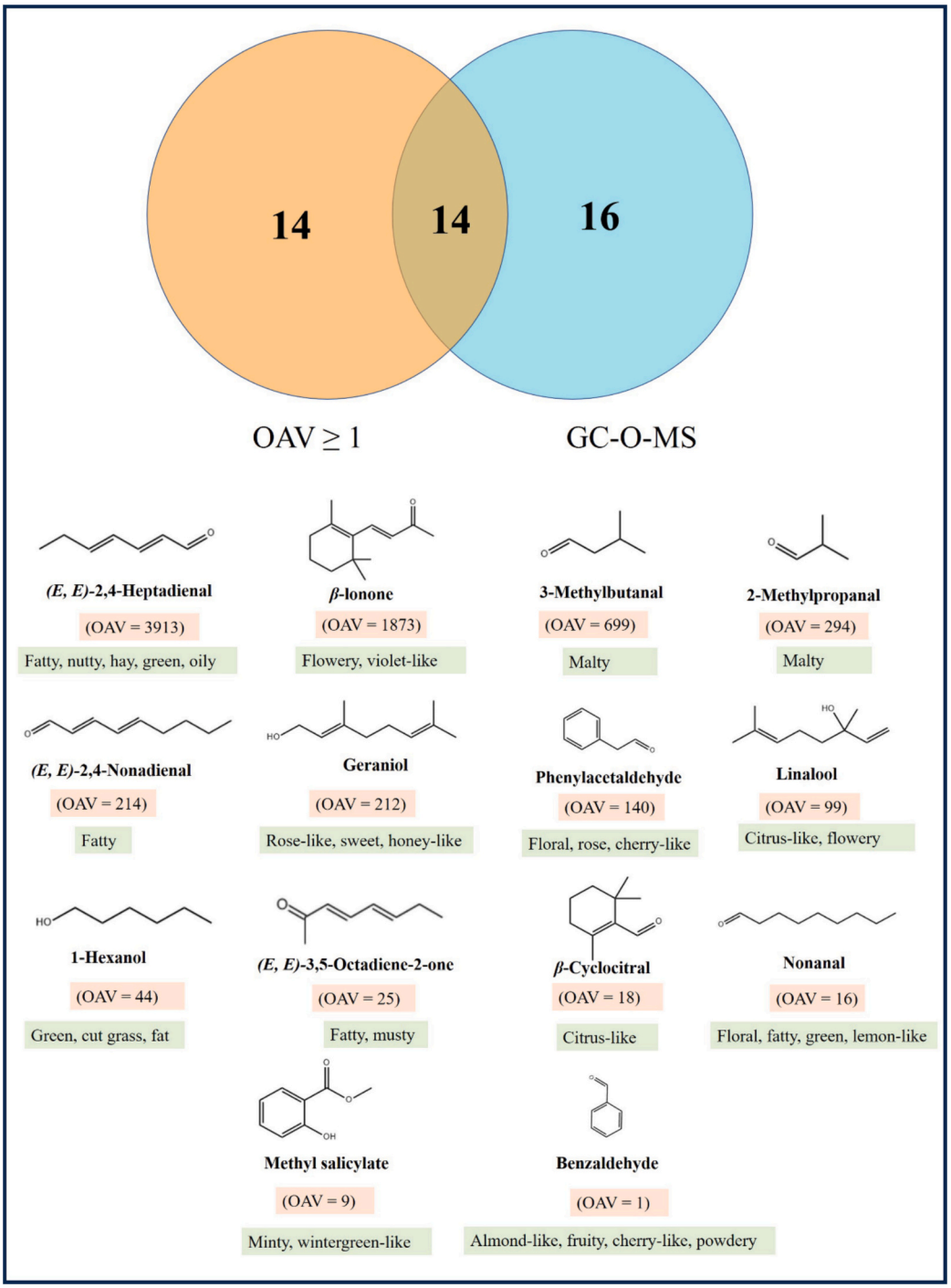

Fig. 5. The key odorants in GOF black tea identified by OAV ≥ 1 and GC-O-MS analysis.

mentioning that *β*-ionone was produced either by enzymatic reactions during fermentation or thermal degradation during the manufacturing process. *β*-Cyclocitral reached the maximum during the fermentation stage while *β*-ionone showed minimal changes throughout processing. These compounds were generally responsible for the characteristic floral and fruity aromas (Guo et al., 2021) (Fig. 6[A] and Fig. 6[B]).

AADVs such as 2-methylpropanal, 3-methylbutanal and phenylacetaldehyde are classified as Strecker aldehydes. The precursors of these three volatiles were valine, leucine, and phenylalanine, respectively (Ho et al., 2015). They were primarily formed via the Maillard reaction during heating processes, especially the reaction of free amino acids with *α*-dicarbonyls (Yin et al., 2022). 2-Methylpropanal and 3-methylbutanal were reported to have a malty flavor while phenylacetaldehyde exhibited floral, rose, and cherry-like flavors (Zhu, Niu, & Xiao, 2021). 3-Methylbutanal steadily increased throughout the processing stages, while 2-methylpropanal and phenylacetaldehyde reached their highest contents during the fermentation stage.

Linalool and geraniol, recognized for their floral and fruity aromas, originated from the geranyl pyrophosphate (geranyl-PP) precursor catalyzed by linalool synthase and geraniol synthase, respectively (Ni et al., 2021). In the whole process, linalool reached the maximum in the withering stage but gradually decreased thereafter, while geraniol exhibited an overall increasing trend from fresh leaves to the first drying stage followed by a decline. In addition, some non-alcoholic odorants

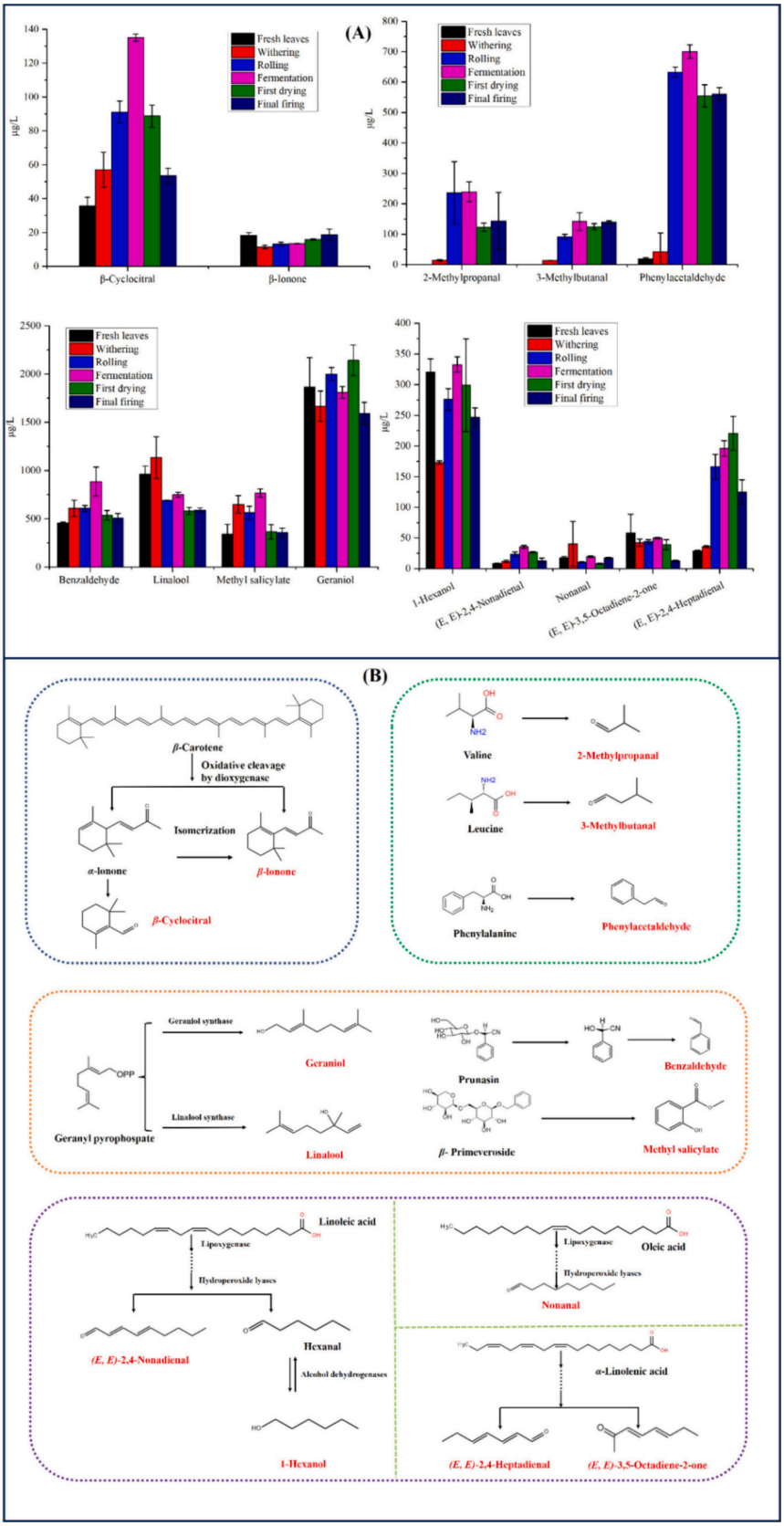

Fig. 6. The dynamic changes and formation pathways of key odorants in GOF black tea. (A) Dynamic changes; (B) Possible formation pathways.

such as benzaldehyde and methyl salicylate were also typically in their glycosidically bound state, and their release necessitated intricate processes. For instance, the liberation of benzaldehyde from prunasin typically involved the mandelonitrile intermediate and subsequent isomerization from acid to aldehyde (Ho et al., 2015). Benzaldehyde showed a significant upward trend after fermentation, and was linked to almond-like, fruity, cherry-like, and nutty flavors. Methyl salicylate, renowned for its minty and wintergreen-like odors, was released from β-primeveroside. Its content attained the maximum during the fermentation stage and subsequently declined precipitously.

The key odorants derived from the lipid degradation pathway primarily comprised some short-chain C6 ~ C9 aliphatic aldehydes (such as nonanal, *(E, E)*-2,4-heptadienal, and *(E, E)*-2,4-nonadienal), ketone (such as *(E, E)*-3,5-octadiene-2-one), and alcohol (such as 1-hexanol). For example, 1-hexanol was derived from the oxidation of linoleic acid, facilitated by lipoxygenase. The specific formation pathway was as follows: linoleic acid was converted into lipid hydroperoxide under the influence of lipoxygenase, subsequently broken down by hydroperoxide lyase (HPLs) to hexanal, and then reduced to 1-hexanol by alcohol dehydrogenase (ADHs). The formation pathway of *(E, E)*-2,4-nonadienal was similar to that of hexanal. 1-Hexanol, giving a green odor to tea, displayed an increasing trend from withering to fermentation and then decreased. *(E, E)*-2,4-Nonadienal, known for its fatty odor, reached the highest content at the fermentation stage (Zhai, Zhang, Granvogl, Ho, & Wan, 2022). It was reported that *(E, E)*-3,5-octadiene-2-one and *(E, E)*-2,4-heptadienal were formed from α-linolenic acid while nonanal was formed from oleic acid (Bhowmik et al., 2023). *(E, E)*-3,5-Octadiene-2-one was associated with creamy and fruity flavors, which showed a consistent decline throughout processing. Nonanal and *(E, E)*-2,4-heptadienal were known for their fatty, green, and oily aromas (Flaig, Qi, Wei, Yang, & Schieberle, 2020). Their contents reached the highest at the withering and first firing stages, respectively.

4. Conclusions

In this study, the key odorants causing GOF in black tea were sought to gain by combining GC-*E*-Nose, GC-IMS, GC-O-MS and GC–MS, and the dynamic changes and formation pathways of volatile profiles were in-depth understood. A total of 79 and 77 volatile components were identified through GC-IMS and GC–MS, respectively. The volatile metabolites of GOF black tea exhibited substantial changes throughout the processing, notably during the withering stage. The analyses of OAV and GC-O-MS confirmed that 14 key odorants including 2-methylpropanal, 3-methylbutanal, 1-hexanol, nonanal, *(E, E)*-2,4-heptadienal, benzaldehyde, linalool, *(E, E)*-3,5-octadiene-2-one, β-cyclocitral, phenylacetaldehyde, *(E, E)*-2,4-nonadienal, methyl salicylate, geraniol, and β-ionone were responsible for GOF. Notably, *(E, E)*-2,4-heptadienal (OAV = 3913), renowned for its fatty, green, and oily aromas, was considered as the most crucial odorant causing GOF. In addition, this investigation unveiled lipid degradation as the primary metabolic pathway underlying the GOF of black tea. To some extent, this study provides theoretical support for improving the quality of black tea. In future, the interaction of these key odorants and pivotal regulatory factors will be further studied, aiming to provide technical reserve for the high-quality development of the black tea industry.

CRediT authorship contribution statement

Yanqin Yang: Writing – review & editing, Writing – original draft, Visualization, Validation, Supervision, Software, Resources, Methodology, Investigation, Funding acquisition, Formal analysis, Data curation, Conceptualization. **Jialing Xie:** Software, Methodology. **Lilei Wang:** Visualization, Resources. **Yan Shang:** Resources. **Yongwen Jiang:** Supervision, Project administration, Funding acquisition. **Haibo Yuan:** Supervision, Project administration, Funding acquisition.

Declaration of competing interest

The authors declare that they have no known competing financial interests or personal relationships that could have appeared to influence the work reported in this paper.

Data availability

Data will be made available on request.

Acknowledgments

This research was supported by Zhejiang Provincial Natural Science Foundation of China (Grant No. LY24C160002), Science and Technology Innovation Project of the Chinese Academy of Agricultural Sciences (Grant No. CAAS-ASTIP-TRICAAS) and China Agriculture Research System of MOF and MARA (Grant No. CARS-19).

Appendix A. Supplementary data

Supplementary data to this article can be found online at https://doi.org/10.1016/j.fochx.2024.101432.

References

Bhowmik, P., Yan, W., Hodgins, C., Polley, B., Warkentin, T., Nickerson, M., … Aliani, M. (2023). CRISPR/Cas9-mediated lipoxygenase gene-editing in yellow pea leads to major changes in fatty acid and flavor profiles. *Frontiers in Plant Science, 14*, Article 1246905. https://doi.org/10.3389/fpls.2023.1246905

Chen, J., Yang, Y., Deng, Y., Liu, Z., Xie, J., Shen, S., … Jiang, Y. (2022). Aroma quality evaluation of Dianhong black tea infusions by the combination of rapid gas phase electronic nose and multivariate statistical analysis. *LWT, 153*, Article 112496. https://doi.org/10.1016/j.lwt.2021.112496

Chen, J.-N., Zhang, Y.-Y., Huang, X.-H., Dong, M., Dong, X.-P., Zhou, D.-Y., … Qin, L. (2023). Integrated volatolomics and metabolomics analysis reveals the characteristic flavor formation in Chouguiyu, a traditional fermented mandarin fish of China. *Food Chemistry, 418*, Article 135874. https://doi.org/10.1016/j.foodchem.2023.135874

Chen, Q., Zhu, Y., Liu, Y., Liu, Y., Dong, C., Lin, Z., & Teng, J. (2022). Black tea aroma formation during the fermentation period. *Food Chemistry, 374*, Article 131640. https://doi.org/10.1016/j.foodchem.2021.131640

Fang, X., Liu, Y., Xiao, J., Ma, C., & Huang, Y. (2023). GC–MS and LC-MS/MS metabolomics revealed dynamic changes of volatile and non-volatile compounds during withering process of black tea. *Food Chemistry, 410*, Article 135396. https://doi.org/10.1016/j.foodchem.2023.135396

Flaig, M., Qi, S., Wei, G., Yang, X., & Schieberle, P. (2020). Characterization of the key odorants in a high-grade Chinese green tea beverage (*Camellia sinensis*; Jingshan cha) by means of the Sensomics approach and elucidation of odorant changes in tea leaves caused by the tea manufacturing process. *Journal of Agricultural and Food Chemistry, 68*(18), 5168–5179. https://doi.org/10.1021/acs.jafc.0c01300

Guo, X., Ho, C.-T., Wan, X., Zhu, H., Liu, Q., & Wen, Z. (2021). Changes of volatile compounds and odor profiles in Wuyi rock tea during processing. *Food Chemistry, 341*, Article 128230. https://doi.org/10.1016/j.foodchem.2020.128230

Guo, X., Schwab, W., Ho, C.-T., Song, C., & Wan, X. (2022). Characterization of the aroma profiles of oolong tea made from three tea cultivars by both GC-MS and GC-IMS. *Food Chemistry, 376*, Article 131933. https://doi.org/10.1016/j.foodchem.2021.131933

Ho, C.-T., Zheng, X., & Li, S. (2015). Tea aroma formation. *Food Science and Human Wellness, 4*(1), 9–27. https://doi.org/10.1016/j.fshw.2015.04.001

Li, X., Zeng, X., Song, H., Xi, Y., Li, Y., Hui, B., … Li, J. (2023). Characterization of the aroma profiles of cold and hot break tomato pastes by GC-O-MS, GC × GC-O-TOF-MS, and GC-IMS. *Food Chemistry, 405*, Article 134823. https://doi.org/10.1016/j.foodchem.2022.134823

Liu, Y., Chen, Q., Liu, D., Yang, L., Hu, W., Kuang, L., … Liu, Y. (2023). Multi-omics and enzyme activity analysis of flavour substances formation: Major metabolic pathways alteration during congou black tea processing. *Food Chemistry, 403*, Article 134263. https://doi.org/10.1016/j.foodchem.2022.134263

Liu, Z., Chen, F., Sun, J., & Ni, L. (2022). Dynamic changes of volatile and phenolic components during the whole manufacturing process of Wuyi rock tea (Rougui). *Food Chemistry, 367*, Article 130624. https://doi.org/10.1016/j.foodchem.2021.130624

Ni, H., Jiang, Q., Lin, Q., Ma, Q., Wang, L., Weng, S., … Chen, F. (2021). Enzymatic hydrolysis and auto-isomerization during β-glucosidase treatment improve the aroma of instant white tea infusion. *Food Chemistry, 342*, Article 128565. https://doi.org/10.1016/j.foodchem.2020.128565

Rong, Y., Xie, J., Yuan, H., Wang, L., Liu, F., Deng, Y., … Yang, Y. (2023). Characterization of volatile metabolites in Pu-erh teas with different storage years by combining GC-E-nose, GC–MS, and GC-IMS. *Food Chemistry: X, 18*, Article 100693. https://doi.org/10.1016/j.fochx.2023.100693

Uselmann, V., & Schieberle, P. (2015). Decoding the combinatorial aroma code of a commercial Cognac by application of the Sensomics concept and first insights into differences from a German brandy. *Journal of Agricultural and Food Chemistry, 63*(7), 1948–1956. https://doi.org/10.1021/jf506307x

Wan, J., Liu, Q., Ma, C., Muhoza, B., Huang, Y., Sun, M., … Ho, C.-T. (2023). Characteristic flavor fingerprint disclosure of dzo beef in Tibet by applying SAFE-GC-O-MS and HS-GC-IMS technology. *Food Research International, 166*, Article 112581. https://doi.org/10.1016/j.foodres.2023.112581

Wang, L., Xie, J., Deng, Y., Jiang, Y., Tong, H., Yuan, H., & Yang, Y. (2023). Volatile profile characterization during the drying process of black tea by integrated volatolomics analysis. *LWT, 184*, Article 115039. https://doi.org/10.1016/j.lwt.2023.115039

Wei, G., Dan, M., Zhao, G., & Wang, D. (2023). Recent advances in chromatography-mass spectrometry and electronic nose technology in food flavor analysis and detection. *Food Chemistry, 405*, Article 134814. https://doi.org/10.1016/j.foodchem.2022.134814

Xiao, Y., Huang, Y., Chen, Y., Xiao, L., Zhang, X., Yang, C., … Wang, Y. (2022). Discrimination and characterization of the volatile profiles of five Fu brick teas from different manufacturing regions by using HS–SPME/GC–MS and HS–GC–IMS. *Current Research in Food Science, 5*, 1788–1807. https://doi.org/10.1016/j.crfs.2022.09.024

Xie, J., Wang, L., Deng, Y., Yuan, H., Zhu, J., Jiang, Y., & Yang, Y. (2023). Characterization of the key odorants in floral aroma green tea based on GC-E-nose, GC-IMS, GC-MS and aroma recombination and investigation of the dynamic changes and aroma formation during processing. *Food Chemistry, 427*, Article 136641. https://doi.org/10.1016/j.foodchem.2023.136641

Yang, Y., Zhang, M., Yin, H., Deng, Y., Jiang, Y., Yuan, H., … Wang, J. (2018). Rapid profiling of volatile compounds in green teas using Micro-chamber/thermal extractor combined with thermal desorption coupled to gas chromatography-mass spectrometry followed by multivariate statistical analysis. *LWT, 96*, 42–50. https://doi.org/10.1016/j.lwt.2018.04.091

Yang, Y., Hua, J., Deng, Y., Jiang, Y., Qian, M. C., Wang, J., … Yuan, H. (2020). Aroma dynamic characteristics during the process of variable-temperature final firing of congou black tea by electronic nose and comprehensive two-dimensional gas chromatography coupled to time-of-flight mass spectrometry. *Food Research International, 137*, Article 109656. https://doi.org/10.1016/j.foodres.2020.109656

Yang, Y., Zhang, M., Hua, J., Deng, Y., Jiang, Y., Li, J., … Dong, C. (2020). Quantitation of pyrazines in roasted green tea by infrared-assisted extraction coupled to headspace solid-phase microextraction in combination with GC-QqQ-MS/MS. *Food Research International, 134*, Article 109167. https://doi.org/10.1016/j.foodres.2020.109167

Yang, Y., Qian, M. C., Deng, Y., Yuan, H., & Jiang, Y. (2022). Insight into aroma dynamic changes during the whole manufacturing process of chestnut-like aroma green tea by combining GC-E-nose, GC-IMS, and GC × GC-TOFMS. *Food Chemistry, 387*, Article 132813. https://doi.org/10.1016/j.foodchem.2022.132813

Yang, Y., Zhu, H., Chen, J., Xie, J., Shen, S., Deng, Y., … Jiang, Y. (2022). Characterization of the key aroma compounds in black teas with different aroma types by using gas chromatography electronic nose, gas chromatography-ion mobility spectrometry, and odor activity value analysis. *LWT, 163*, Article 113492. https://doi.org/10.1016/j.lwt.2022.113492

Yang, Y., Wang, Q., Xie, J., Deng, Y., Zhu, J., Xie, Z., … Jiang, Y. (2024). Uncovering the dynamic alterations of volatile components in sweet and floral aroma black tea during processing. *Foods, 13*(5), 728. https://www.mdpi.com/2304-8158/13/5/728.

Yang, Y., Xie, J., Wang, Q., Deng, Y., Zhu, L., Zhu, J., … Jiang, Y. (2024). Understanding the dynamic changes of volatile and non-volatile metabolites in black tea during processing by integrated volatolomics and UHPLC-HRMS analysis. *Food Chemistry, 432*, Article 137124. https://doi.org/10.1016/j.foodchem.2023.137124

Yin, P., Kong, Y.-S., Liu, P.-P., Wang, J.-J., Zhu, Y., Wang, G.-M., … Liu, Z.-H. (2022). A critical review of key odorants in green tea: Identification and biochemical formation pathway. *Trends in Food Science & Technology, 129*, 221–232. https://doi.org/10.1016/j.tifs.2022.09.013

Yin, X., Xiao, Y., Wang, K., Wu, W., Huang, J., Liu, S., & Zhang, S. (2023). Effect of shaking manners on floral aroma quality and identification of key floral-aroma-active compounds in Hunan black tea. *Food Research International, 174*, Article 113515. https://doi.org/10.1016/j.foodres.2023.113515

Zhai, X., Zhang, L., Granvogl, M., Ho, C.-T., & Wan, X. (2022). Flavor of tea (*Camellia sinensis*): A review on odorants and analytical techniques. *Comprehensive Reviews in Food Science and Food Safety, 21*(5), 3867–3909. https://doi.org/10.1111/1541-4337.12999

Zhang, H., Huang, D., Pu, D., Zhang, Y., Chen, H., Sun, B., & Ren, F. (2020). Multivariate relationships among sensory attributes and volatile components in commercial dry porcini mushrooms (boletus edulis). *Food Research International, 133*, Article 109112. https://doi.org/10.1016/j.foodres.2020.109112

Zhao, M., Li, T., Yang, F., Cui, X., Zou, T., Song, H., & Liu, Y. (2022). Characterization of key aroma-active compounds in Hanyuan Zanthoxylum bungeanum by GC-O-MS and switchable GC x GC-O-MS. *Food Chemistry, 385*, Article 132659. https://doi.org/10.1016/j.foodchem.2022.132659

Zhou, Y., He, Y., & Zhu, Z. (2023). Understanding of formation and change of chiral aroma compounds from tea leaf to tea cup provides essential information for tea quality improvement. *Food Research International, 167*, Article 112703. https://doi.org/10.1016/j.foodres.2023.112703

Zhu, J., Niu, Y., & Xiao, Z. (2021). Characterization of the key aroma compounds in Laoshan green teas by application of odour activity value (OAV), gas chromatography-mass spectrometry-olfactometry (GC-MS-O) and comprehensive two-dimensional gas chromatography mass spectrometry (GC × GC-qMS). *Food Chemistry, 339*, Article 128136. https://doi.org/10.1016/j.foodchem.2020.128136